

This article was downloaded by:

On: 26 January 2011

Access details: *Access Details: Free Access*

Publisher *Taylor & Francis*

Informa Ltd Registered in England and Wales Registered Number: 1072954 Registered office: Mortimer House, 37-41 Mortimer Street, London W1T 3JH, UK



Liquid Crystals

Publication details, including instructions for authors and subscription information:

<http://www.informaworld.com/smpp/title~content=t713926090>

Some dynamic features of the preparation of liquid crystalline elastomers

Conor J. Twomey^{ab}, Thomas N. Blanton^c, Kenneth L. Marshall^b, Shaw H. Chen^b, Stephen D. Jacobs^b

^a Department of Chemical Engineering, Gavett Hall, University of Rochester, Rochester, New York, U.S.A. ^b Laboratory for Laser Energetics, University of Rochester, Rochester, New York, U.S.A. ^c

Analytical Technology Division, Eastman Kodak Company, Rochester, New York, U.S.A.

To cite this Article Twomey, Conor J. , Blanton, Thomas N. , Marshall, Kenneth L. , Chen, Shaw H. and Jacobs, Stephen D.(1995) 'Some dynamic features of the preparation of liquid crystalline elastomers', *Liquid Crystals*, 19: 3, 339 — 344

To link to this Article: DOI: 10.1080/02678299508031990

URL: <http://dx.doi.org/10.1080/02678299508031990>

PLEASE SCROLL DOWN FOR ARTICLE

Full terms and conditions of use: <http://www.informaworld.com/terms-and-conditions-of-access.pdf>

This article may be used for research, teaching and private study purposes. Any substantial or systematic reproduction, re-distribution, re-selling, loan or sub-licensing, systematic supply or distribution in any form to anyone is expressly forbidden.

The publisher does not give any warranty express or implied or make any representation that the contents will be complete or accurate or up to date. The accuracy of any instructions, formulae and drug doses should be independently verified with primary sources. The publisher shall not be liable for any loss, actions, claims, proceedings, demand or costs or damages whatsoever or howsoever caused arising directly or indirectly in connection with or arising out of the use of this material.

Some dynamic features of the preparation of liquid crystalline elastomers

by CONOR J. TWOMEY†§, THOMAS N. BLANTON‡,
KENNETH L. MARSHALL*§, SHAW H. CHEN*§ and STEPHEN D. JACOBS§

† Department of Chemical Engineering, Gavett Hall, University of Rochester,
Rochester, New York 14627-0166, U.S.A.

‡ Analytical Technology Division, Kodak Park, Bldg. 49 Eastman
Kodak Company, Rochester, New York 14652-3712, U.S.A.

§ Laboratory for Laser Energetics, University of Rochester, 250 East River Road,
Rochester, New York 14623-1299, U.S.A.

(Received 15 August 1994; in final form 14 February 1995; accepted 21 February 1995)

Liquid crystalline elastomers derived from siloxane polymers, PMHS and PEHS, were prepared following a two-stage reaction scheme to investigate the effects of processing conditions and thermal treatment on mesomorphic characteristics. The LC elastomer samples were analysed by FTIR, DSC, stress-strain relationship, polarized optical microscopy, and X-ray diffraction techniques. Key findings include: (1) Chain length of the precursor siloxane polymer is critical to achieving a bulk alignment via stretching during the second-stage reaction; (2) the imposed strain is also critical to achieving a monodomain nematic character, which is completely recoverable upon heating beyond the clearing temperature followed by cooling back to room temperature (i.e. thermal treatment); (3) enthalpy is stored in an elastomer freshly prepared without an imposed strain, but the imposed strain helps to release the stored enthalpy, which can be almost completely released upon thermal treatment; and (4) while the stored enthalpy does not increase order parameter (HOF_A), its release through molecular relaxation contributes to an increased HOF_A value.

1. Introduction

Liquid crystalline, LC, polymers have been the focus of intensive research in recent years largely because of the potential for a wide range of optical as well as photonic applications [1–3]. The macroscopic alignment desired for practical applications can be achieved by surface treatment and the application of an external electric or magnetic field. Nevertheless, the effectiveness of these processing techniques is limited to films with a thickness less than 100 μm [4]. To overcome this problem, liquid crystalline elastomers have been explored in view of the relative ease with which alignment of mesogenic moieties can be accomplished by stretching [5–11]. However, the stress-induced macroscopic order will diminish as the applied stress is relaxed.

To obviate the need for sustained stresses, Finkelmann *et al.* [12], have introduced a novel two-stage reaction scheme for the preparation of LC elastomers. In the first stage, a hydrosilylation reaction on terminal methylene groups was accomplished to obtain a lightly crosslinked

elastomer carrying two pendant groups: a nematogen and a methacrylate. In the second stage, a constant stress was applied to achieve the nematic alignment followed by further crosslinking through the less reactive methacryloyl groups. This second stage reaction locks in the stress-induced alignment. We note that poly(methylhydrosiloxane), PMHS, with a degree of polymerization, n , of 120 was employed.

In the present work we examined the effects of processing conditions, chain length of precursor siloxane polymer, and thermal treatment on mesomorphic characteristics of LC elastomers. Instead of a constant stress, as imposed by Finkelmann *et al.* [12], a constant strain was imposed during the second stage reaction. Commercially available PMHS and poly(ethylhydrosiloxane), PEHS, with an n value of 40 and 80, respectively, were employed in the preparation of elastomers. It is noted that PMHS with an n value of 40 as opposed to 120 requires a higher degree of crosslinking, 13 mol % versus 5% of crosslinkers in the formulation, to obtain a reasonably stretchable sample after the first-stage reaction. The resultant elastomers were characterized with Fourier transform infrared (FTIR) spectroscopy, differential scanning calorimetry

* Authors for correspondence.

(DSC), hot stage polarized optical microscopy, stress-strain analysis, and the X-ray techniques.

2. Experimental

2.1. Materials

Poly(methylhydrosiloxane), PMHS, $-\text{[(CH}_3\text{)SiH-O]}_{40}-$, (0.30 Stoke, Spectrum Chemicals), poly(ethylhydrosiloxane), PEHS, $-\text{[(C}_2\text{H}_5\text{)SiH-O]}_{80}-$, (1.00 Stoke, Gelest), toluene (anhydrous, +99 per cent Aldrich Chemical Company), and a Pt-catalyst (PC072, United Chemical Technologies) were all used as received without further purification.

2.2. Preparation of elastomers

The nematic monomer (NM), and 1st crosslinking agent (C1), and the 2nd crosslinking agent (C2), as shown in figure 1, were synthesized according to standard literature methods ([12] and references cited therein). To prepare the elastomers appropriate quantities of NM, C1 and C2 were added to PEHS or PMHS in a round-bottomed reaction flask to ensure a polymer:NM:C1:C2 molar ratio of 1:0.3:0.1:0.1. Upon addition of toluene (13.6 ml/g-material), the flask was sealed, flushed with nitrogen, and heated to ensure dissolution of solids. Then the catalyst was added ($[\text{Pt/CH}_2=\text{CH-}] \approx 0.002$), and the flask shaken vigorously for 30 s before quickly transferring the contents to a heated teflon mould kept at 60°C under a nitrogen purge overnight (i.e. the first-stage reaction). Afterwards, the elastomer was carefully removed from the mould, stretched by the desired amount, and left on a hot plate set at 60°C for 3 d to complete the elastomer preparation (i.e. the second-stage reaction). The

extent of reaction was monitored using FTIR spectroscopy. The elastomers prepared from PEHS and PMHS are denoted as ES and MS, respectively in what follows.

2.3. Methods of characterization

The degrees of polymerization of PEHS and PMHS were evaluated from a viscosity versus molecular weight relationship derived from product data (United Chemical Technologies). Infrared spectra were taken of free standing films and thin elastomer films prepared on NaCl plates using a Nicolet 20SXC FTIR spectrophotometer with a precision of $\pm 0.2 \text{ cm}^{-1}$. Thermal data were collected using a Perkin-Elmer DSC-4 at $+20^\circ\text{C min}^{-1}$ under a helium purge. The inflection point on the DSC thermogram is reported as T_g . A hot stage polarized optical microscope (Leitz Orthoplan-Pol and a Mettler FP52 Microthermal System) was used for mesophase identification and verification of transition temperatures determined with DSC. Mechanical characterization of elastomers was conducted in a water bath at $55 \pm 1^\circ\text{C}$ using an Instron Table Model 1102 instrument. The stress, σ , is determined in terms of the original cross-sectional area, and the strain defined as $\varepsilon = (l - l_0)/l_0$, where l and l_0 are the length at the time of data collection and original length, respectively.

Two-dimensional flat plate X-ray diffraction patterns were collected using a Statton box camera with a sample-to-film distance of 5.0 cm. An image plate storage phosphor detector was utilized in place of X-ray film to reduce data collection time [13]. Samples were irradiated with nickel filtered copper radiation. A qualitative assessment of orientation and liquid crystallinity was accomplished using the flat plate diffraction data. The X-ray diffraction patterns were obtained with a Rigaku RU-300 pole figure goniometer operated in the Bragg-Brentano geometry. This diffractometer was equipped with a copper rotating anode operated at 50 kV and 280 mA, diffracted beam nickel filter, and a scintillation detector. Reflection mode $\theta/2\theta$ scans provided information on planar orientation. Symmetrical transmission mode $\theta/2\theta$ scans provided a preliminary assessment of in-plane orientation. A quantitative orientation analysis was performed using an azimuthal diffraction technique [14]. Data were collected with the Rigaku RU-300 pole goniometer as mentioned above. Azimuthal analysis involved positioning a sample at a fixed θ in the symmetric transmission mode with the detector at a fixed 2θ to detect a desired Bragg diffraction peak. The sample is then rotated 360° around the normal to the sample plane, defined as the χ rotation. In this study the transverse direction was mounted at zero azimuthal angle, i.e. parallel to the plane of the X-ray beam. Orientation distribution was quantified by the use of the Herman's orientation distribution function (HOF_A) defined for in-plane alignments as [14]

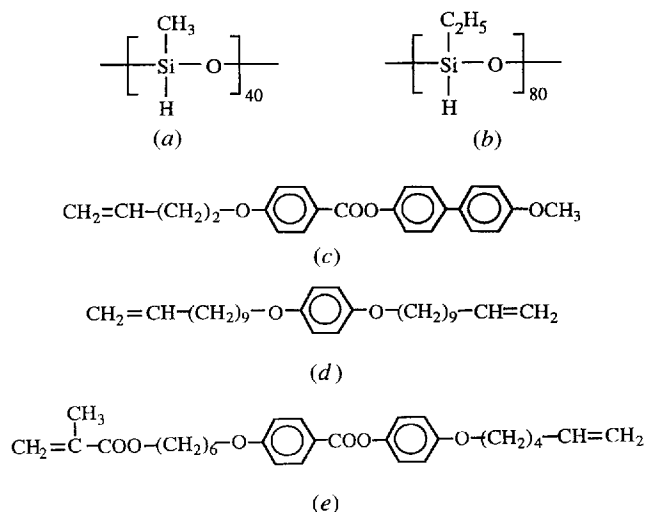


Figure 1. Materials used in the preparation of the liquid crystalline elastomers: (a) poly(methylhydrosiloxane); (b) poly(ethylhydrosiloxane); (c) nematic monomer; (d) 1st crosslinking agent; and (e) 2nd crosslinking agent.

$$\text{HOF}_A = \frac{3\langle \cos^2 \chi \rangle - 1}{2} \quad (1)$$

with $\langle \cos^2 \chi \rangle$ defined as

$$\langle \cos^2 \chi \rangle = \frac{\sum I(\chi) \sin \chi \cos^2 \chi}{\sum I(\chi) \sin \chi} \quad (2)$$

where $I(\chi)$ denotes intensity as a function of azimuthal angle, χ (see figure 7). Note that the value of HOF_A ranges from -0.5 to 1 for in-plane orientation distribution, with a value of -0.5 indicating a perfect alignment of polymer chains along the machine direction, a value of 0 indicating a random or balanced alignment, and a value of 1 indicating a perfect alignment of polymer chains along the transverse direction [14].

3. Results and discussion

In the elastomer synthesis, FTIR was used to monitor the hydrosilylation reaction as illustrated in figure 2 for MS where a comparison of scans recorded after the first-stage (2 (a)) and second-stage (2 (b)) reaction show the expected reduction in the intensity of the Si-H stretching band at 2160 cm^{-1} . The effect of reaction on the mechanical properties of ES and MS is illustrated in figure 3. In light of the reported effect of crosslink density on glass transition and clearing temperatures [4–11], it is important to ensure that a valid comparison of ES to MS is made. The crosslink density in terms of the molecular weight between crosslinks, M_c , is related to the elastic modulus, E (N mm^{-2}), at low strains and temperatures above T_g by equation (3) [6]:

$$E = \frac{3\rho RT}{M_c} \quad (3)$$

where ρ is the density estimated at 1.0 g cm^{-3} [8, 11], R the ideal gas constant, and T the temperature ($^\circ\text{K}$). Since the data were collected at 55°C (i.e. above the T_g s determined in figure 4), equation (3) is appropriate for evaluating E from figure 3. Thus, M_c of 660 ($E = 12.4 \text{ N mm}^{-2}$) and 560 g mol^{-1} ($E = 14.6 \text{ N mm}^{-2}$) were found for ES and MS elastomers, respectively. Also, we note that figure 3 shows the expected increase in E (i.e. a decrease in M_c) with an increased extent of reaction. Since stretching of samples during the second-stage reaction is required to achieve bulk alignment of the nematic moieties, the maximum strain sustained, ε_b , is an important parameter. For our elastomer composition as defined earlier, ES and MS were found to present an ε_b value of 0.31 and 0.16 , respectively. It is believed that the difference in ε_b originates in the higher molecular weight of the ES system. Recall that the degrees of polymerization of the PEHS and PMHS polymers are 80 and 40 , respectively. In what follows, samples referred to as being 'stretched' are those which were strained to their fullest possible extent during the second-stage reaction.

The DSC thermograms of ES and MS are presented in figure 4, where subscripts s and u refer to samples which were stretched and unstretched during the second-stage reaction, respectively. The T_g s of PEHS and PMHS are -149 and -140°C , respectively, as determined using DSC. Therefore, the reaction (i.e. substitution and crosslinking) elevates the T_g s of both polymer hosts, consistent with the increase in E observed in figure 3. In the first heating scans of ES and MS elastomers, endotherms were observed at 82°C (see figure 4 (a)) and

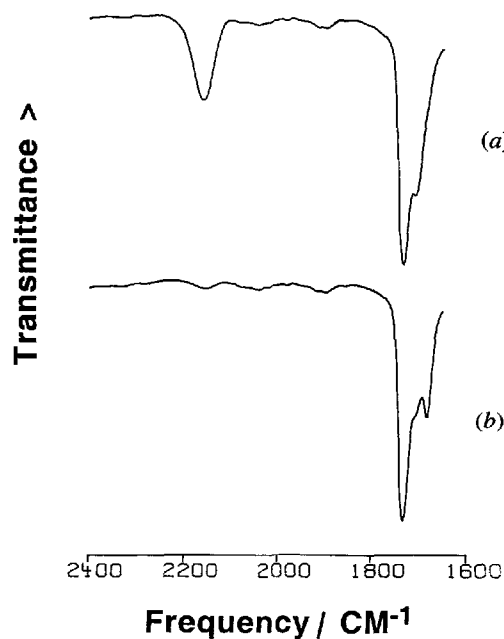


Figure 2. FTIR spectra of MS elastomer after (a) first-stage and (b) second-stage reaction.

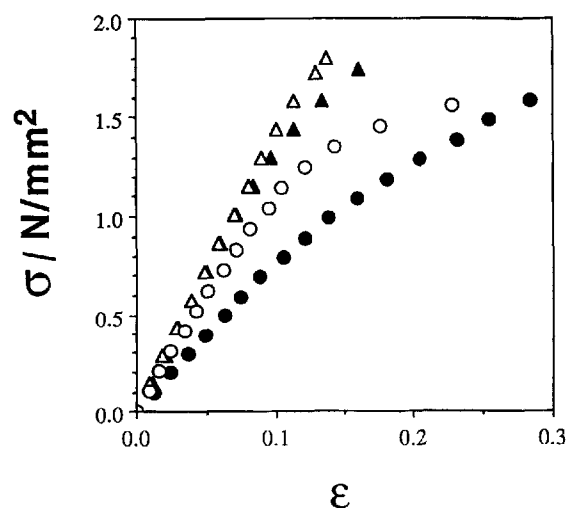


Figure 3. Stress (σ) versus strain (ε) recorded at 55°C for MS elastomer after 1st-stage (\blacktriangle) and 2nd-stage reaction (\triangle), and ES elastomer after 1st-stage (\bullet) and 2nd-stage reaction (\circ).

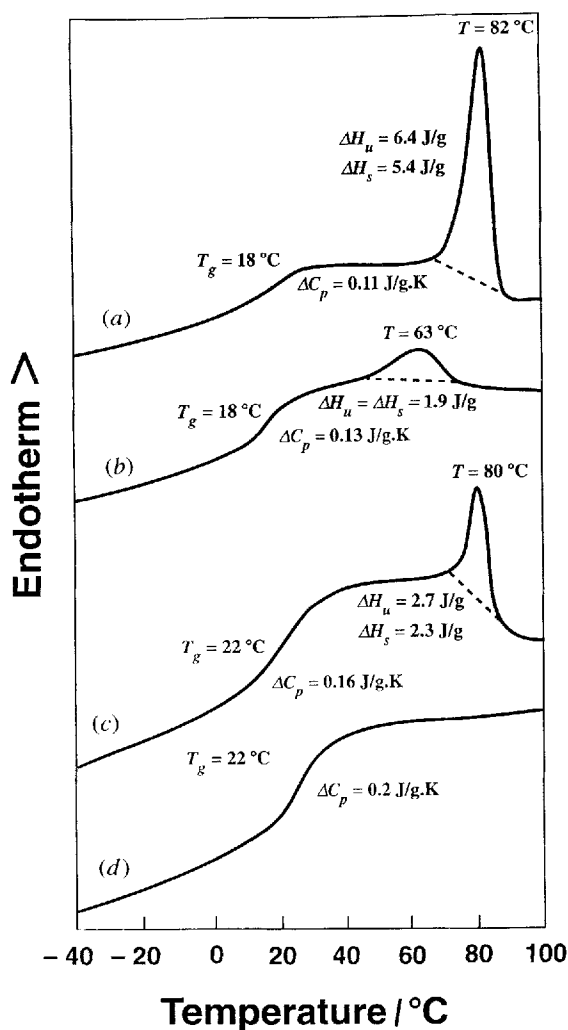


Figure 4. DSC thermograms recorded at $20^\circ\text{C min}^{-1}$ of (a) ES elastomer; (b) second heating scan of ES elastomer first heated to 90°C before cooling at 5°C min^{-1} to room temperature; (c) MS elastomer; and (d) second heating scan of MS elastomer heated to 90°C before cooling at 5°C min^{-1} to room temperature.

80°C (see figure 4(c)) with enthalpies decreasing upon stretching. Between T_g and T_c , nematic textures were identified under polarized optical microscopy for both ES and MS. However, the observed values of ΔH_u and ΔH_s are both greater than can be properly accounted for by a typical nematic to isotropic transition, suggesting another on-going process during the first heating scan, as will be revisited below. After heating the ES sample through the transition temperature (i.e. 82°C) and slowly cooling to room temperature, an endotherm appears at 63°C instead (see figure 4(b)) with a diminished enthalpy of transition. This endotherm represents a nematic to isotropic transition (i.e. $\Delta H_u = \Delta H_s = \Delta H_{n-i}$). Additionally, when an ES elastomer is quenched from 90°C followed by annealing at 60°C , subsequent heating gives an endotherm at 70°C

with an enthalpy of transition of 1.9 J g^{-1} , identical to the value shown in figure 4(b). Thus, while the enthalpy of clearing appears to be independent of thermal history, the clearing temperature does appear to be dependent. The absence of an endotherm in figure 4(d) for MS upon heating to 90°C followed by cooling to room temperature suggests a loss of nematic ordering. In contrast, Finkelmann *et al.* [12], reported values for T_g , T_{N-I} , and ΔH_{N-I} of 0°C , 83°C , and 1.7 J g K^{-1} , respectively, for the elastomer prepared from PMHS with a degree of polymerization of 120. Other than differences in the chain length of the starting PMHS and in the crosslink density, no explanation can be offered for the discrepancy with our experimental results.

Before further probing the endotherm visible during the first heating scans of ES and MS, let us explore molecular orientation using the X-ray technique. The flat plate diffraction pattern for the unstretched ES sample (see figure 5(a)) shows two broad diffraction rings characteristic of a polydomain nematic, as was also observed for the unstretched MS elastomer. Interplanar spacing calculations reveal that the inner and outer rings have d -spacings of 8.8 and 4.38 \AA , respectively. Upon stretching the elastomers, in-plane orientation occurs as evidenced by the formation of arcs in the flat plate diffraction pattern for the ES elastomer with $\epsilon = 0.3$ (see figure 5(b)), which is characteristic of a monodomain nematic [15]. Due to the lower sustainable strains in the MS elastomer (see figure 3); the effect of strain on orientation in this system is not pronounced. Hence, we focus our attention on the ES sample with a note that the majority of the diffraction scatter lies in the equatorial position (zeroth order) in the flat plate pattern which indicates that the 8.8 and 4.38 \AA diffraction peaks are of the type $(hk0)$. In the following discussion, 'thermal treatment' refers to the process whereby samples are heated at 90°C for 10 min and then cooled to room temperature. Upon thermal treatment of the stretched ES, the nematic order is retained, as evidenced by the absence of any discernible effect on arc formation (compare figures 5(b) and 5(c)).

To identify the other process occurring simultaneously with the nematic to isotropic transition during the first heating scans of ES and MS (in the DSC experiment), let us examine the transmission mode diffraction data, as shown in figure 6 over a selected range of 2θ for ES. An inspection of figure 6 reveals that for both unstretched (Ia) and stretched (IIa) ES samples, the 4.38 \AA peak (corresponding to the outer ring shown in figure 5) observed in the flat plate diffraction data actually comprises two peaks with d -spacings of 4.47 and 4.13 \AA . The ability to reveal the presence of two peaks is due to the 20 cm sample-to-detector distance, compared to 5 cm utilized in the flat plate diffraction work. It is evident that the intensity of the 4.13 \AA peak relative to that of the 4.47 \AA peak is

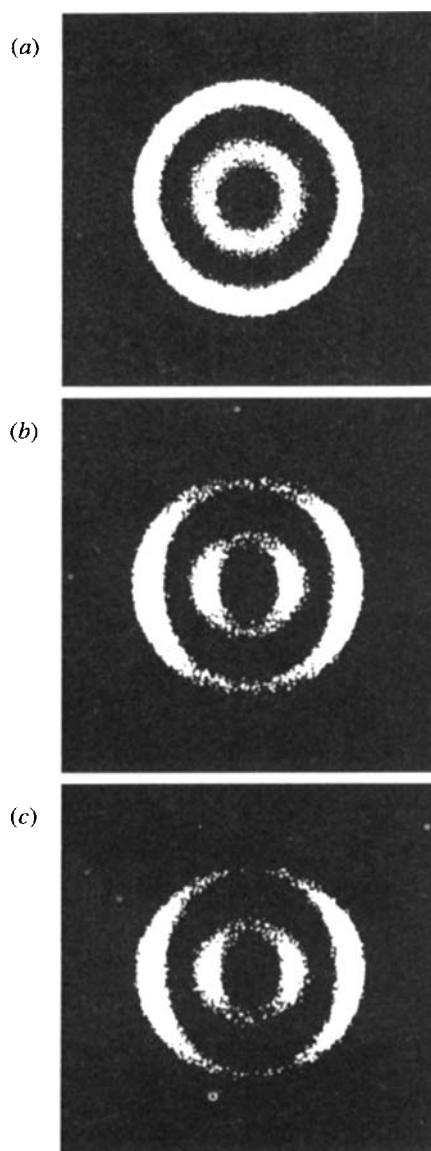


Figure 5. Flat plate X-ray diffraction patterns of ES elastomer: (a) unstretched; (b) stretched to $\epsilon = 0.3$; and (c) as in (b) but first heated to 90°C and then cooled to room temperature.

diminished by stretching. Moreover, the 4.13 \AA peak disappears with an increase in intensity of the 4.47 \AA peak with thermal treatment, as revealed in comparing *Ib* to *Ia* and *IIb* to *IIa*. These observations indicate that stretching and thermal treatment may induce some degree of molecular relaxation, consistent with the facts that $\Delta H_u > \Delta H_s$ and that ΔH_u and ΔH_s both decrease to 1.9 J g^{-1} upon thermal treatment (see figure 4).

Azimuthal diffraction data collected on the 4.47 \AA peak, as shown in figure 7, permits a quantitative assessment of molecular relaxation resulting in an enhanced order reflected by the HOF_A parameter defined by equation (1). These data reveal that the unstretched ES sample has no

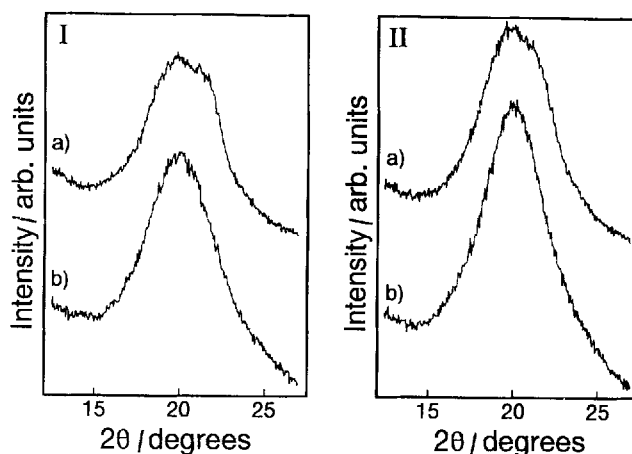


Figure 6. X-ray diffraction patterns of ES elastomer: (Ia) unstretched; (b) sample I upon heating at 90°C for 10 min followed by cooling to room temperature; IIa stretched to $\epsilon = 0.3$; (II b) as in (II a) upon heating at 90°C .

in-plane alignment, indicating a near random distribution of lattice planes based on a HOF_A value of 0.02 in agreement with figure 5 (a). For the stretched ES sample, the peaks at 0° and 180° azimuthal positions in figure 7 (along the sample transverse direction) and a HOF_A value of 0.35 quantify the effect of stretching on the preferred orientation of (*hk*0) lattice planes. Thermal treatment of the stretched sample shows an enhancement of the azimuthal intensity along the transverse direction, resulting in an increased HOF_A value of 0.43 apparently due to the alignment of nematic domains. These observations also support the flat plate diffraction data shown in figures 5 (b) and 5 (c) where the increased order upon thermal

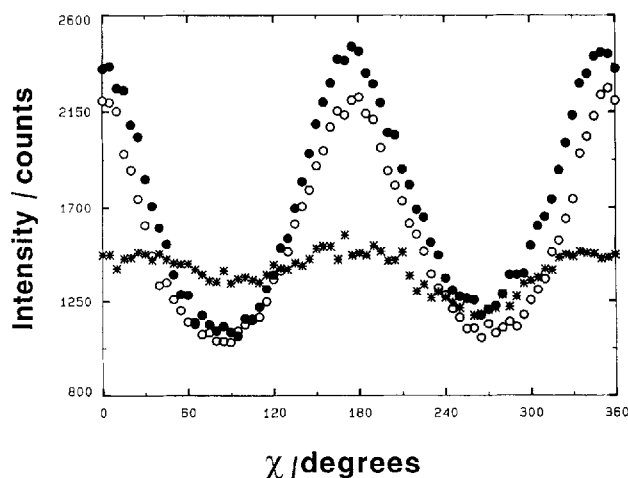


Figure 7. X-ray diffraction azimuth plots for ES elastomer at $2\theta = 19.8^\circ$, i.e. the 4.47 \AA peak in figure 6: (*) unstretched, (○) stretched to $\epsilon = 0.3$, and (●) stretched to $\epsilon = 0.3$ while heating at 90°C for 10 min followed by cooling to room temperature.

treatment is not as apparent. To be consistent with the observed order in which the HOF_A value increases upon stretching and thermal treatment, the DSC thermograms a and b in figure 4 can be interpreted in terms of enthalpy stored at the molecular scale that is released to some extent by stretching during the second-stage reaction and completely released by thermal treatment.

4. Conclusions

Liquid crystalline elastomers were prepared following a two-stage reaction scheme under a constant strain condition using commercially available siloxane polymers PMHS and PEHS with a degree of polymerization (n) of 40 and 80, respectively. Under otherwise identical conditions, the greater n value appears to enable a monodomain characteristic to be achieved by permitting a greater strain to be imposed during the second-stage reaction. Investigations on the elastomer derived from PEHS lead to the following main conclusions:

(i) Based on the flat plate X-ray diffraction pattern, an imposed strain gives rise to a monodomain nematic characteristic, whereas a polydomain characteristic is observed without strain. Furthermore, the monodomain characteristic achieved with strain is retained upon heating beyond the clearing temperature followed by cooling back to room temperature.

(ii) The DSC thermograms coupled with the transmission mode X-ray diffraction data suggest that enthalpy is stored in the freshly prepared elastomer, that the imposed strain helps to release the stored enthalpy to some extent, and that the stored enthalpy is almost completely released upon heating beyond the clearing temperature followed by cooling back to room temperature.

(iii) From the transmission mode and azimuthal X-ray diffraction data, it is concluded that while the stored enthalpy does not lead to an increased order parameter (HOF_A), the enthalpy is released through molecular relaxation upon stretching or thermal treatment, thereby contributing to enhanced nematic ordering with increased HOF_A values.

This work was supported in part by the Army Research Office under Contract #DAAL03-92-G-0147, the Contact Lens Division of Bausch and Lomb, Inc., the U.S.

Department of Energy Office of Inertial Confinement under Cooperative Agreement No. DE-FC03-92SF19460, and the University of Rochester. The support of DOE does not constitute an endorsement by DOE of the views expressed in this article. The authors would like to thank Craig Barnes of Eastman Kodak Company for assistance in gathering the X-ray data, Eric J. Leibenguth and Linda Slapelis of Bausch and Lomb for assistance in the stress-strain analysis, Dr Jay F. Kunzler of Bausch and Lomb for helpful discussions, Darin Phelps of the Department of Chemical Engineering for assistance in monomer synthesis, and Professor Burns of the Department of Mechanical Engineering, University of Rochester for helpful discussions.

References

- [1] (a) FINKELMANN, H., 1987, *Angew. Chem. Int. Ed. Engl.*, **26**, 816; (b) FINKELMANN, H., 1991, *Liquid Crystallinity in Polymers: Principles and Fundamental Properties*, edited by A. Ciferri (VCH Publishers, New York), p. 315.
- [2] GRAY, G. W., 1989, *Side Chain Liquid Crystal Polymers*, edited by B. McArdle (Blackie), p. 106.
- [3] PERCEC, V., and ZHENG, Q., 1992, *J. Mater. Chem.*, **2**, 475.
- [4] SCHATZLE, J., and FINKELMANN, H., 1987, *Molec. Crystals liq. Crystals*, **142**, 85.
- [5] GLEIM, W., and FINKELMANN, H., 1989, *Side Chain Liquid Crystal Polymers*, edited by B. McArdle (Blackie), p. 287.
- [6] DAVIS, F. J., 1993, *J. Mater. Chem.*, **3**, 551.
- [7] BREHMER, M., and ZENTEL, R., 1994, *Molec. Crystals liq. Crystals*, **243**, 353.
- [8] TSUTSUI, T., and TANAKA, R., 1981, *Polymer*, **22**, 117.
- [9] (a) ZENTEL, R., and BENALIA, M., 1987, *Mackromolek. Chem.*, **188**, 665; (b) ZENTEL, R., and RECKERT, G., 1986, *Mackromolek. Chem.*, **187**, 1915.
- [10] LOTH, H., and EUSCHEN, A., 1988, *Makromolek. Chem., rap. Commun.*, **9**, 35.
- [11] (a) KUPFER, J., and FINKELMANN, H., 1994, *Macromol. chem. Phys.*, **195**, 1353; (b) SCHATZLE, J., KAUFHOLD, W., and FINKELMANN, H., 1989, *Makromolek. Chem.*, **190**, 3269; (c) FINKELMANN, H., KOCK, H.-J., and REHAGE, G., 1981, *Makromolek. Chem. rap. Commun.*, **2**, 317.
- [12] KUPFER, J., and FINKELMANN, H., 1991, *Mackromolek. Chem., rap. Commun.*, **12**, 717.
- [13] BLANTON, T. N., *Advances in X-ray Analysis*, Vol. 37 (Plenum Press), (in the press).
- [14] ALEXANDER, L. E., 1969, *X-ray Diffraction Methods in Polymer Science* (Wiley-Interscience).
- [15] FALGUEIRETTES, J., and DELORD, P., 1974, *Liquid Crystals and Plastic Crystals, Vol. 2: Physicochemical Properties and Methods of Investigation*, edited by G. W. Gray and P. A. Winsor (Halsted Press), p. 63.